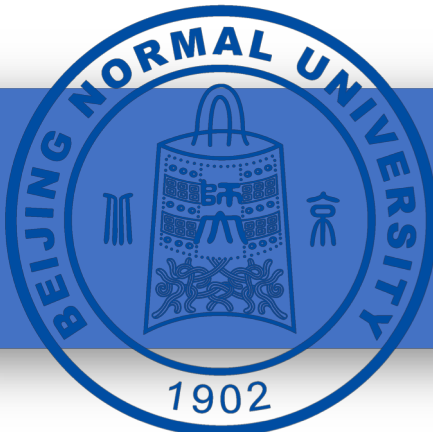


# Agent Based Modeling and Complex Networks Approaches in Human-Nature Coupling Systems study

ASU Sep 09 2019



韩战钢  
zhan@bnu.edu.cn  
北京师范大学系统科学学院



# A Systematic Approach to Uneven CO<sub>2</sub> Distribution and Tele-connection

# $\text{CO}_2$ and tele-connection

- $\text{CO}_2$  is the most important anthropogenic greenhouse gas and the increase of  $\text{CO}_2$  concentrations in the atmosphere is believed to be the primary cause of global warming (IPCC, 2013).
- $\text{CO}_2$  concentrations in 2016 have exceeded the historical 400 parts per million (ppm) (WMO, 2016).
- An improved quantitative understanding of the long-term links of atmospheric  $\text{CO}_2$  are essential for facilitating the study of climate system and reliably predicting future climate.

# Literature

- observations have been expanded to a global network of ground-based flask observations(Wunch et al., 2011; Newman et al., 2016).
- However, in-situ observation networks are sparse in global and regional coverage.
- Continuous measurements from space (Buchwitz et al., 2005; Kuze et al., 2009; Eldering et al., 2017) have the advantages of monitoring global spatial and continuous coverage of greenhouse gases on daily to monthly basis.

# Network Approach

- In the recent decade, with the development of complex network theories, the concept of climate networks has become popular and many research activities have been initiated. Network-based approaches have been applied as a toolbox for analyzing, modelling, understanding, and even predicting climate phenomena (Guez et al., 2014; Gao et al., 2016; Meng et al., 2018).
- In climate networks, nodes represent geographical locations, and communications between different locations are regarded as links.
- The crosscorrelation between records in two locations is one of the most commonly used measures for determining the links between the time series of two nodes (Castrejon-Pita and Read, 2010).

# Data

- AIRS is the first in the new generation of high spectral resolution infrared sounder instruments flown aboard the NASA Aqua satellite mission. The mixing ratios of CO<sub>2</sub> have been retrieved from the spectral channels between 690 and 725 cm<sup>-1</sup> using vanishing partial derivatives (VPD) for clear-sky footprints (Chahine et al., 2005). The maximum sensitivity of AIRS midtropospheric CO<sub>2</sub> retrieval is from 500 to 300 hPa.
- The data in this paper come from NASA's official AIRS mid-troposphere CO<sub>2</sub> retrieval product site ([http://airs.jpl.nasa.gov/AIRS\\_CO2\\_Data/](http://airs.jpl.nasa.gov/AIRS_CO2_Data/)). AIRS mid-tropospheric CO<sub>2</sub> retrievals are available at 2° (latitude) 2.5° (longitude) from September 2002 to present.
- AIRS CO<sub>2</sub> retrieval products are available from 60° S to 90° N over land and ocean, day and night from the Goddard Earth Sciences Data and Information Services Center. Validation against in situ aircraft and retrievals by land-based upward looking Fourier Transform Interferometers demonstrates an accuracy of 1-2 ppm for individual retrievals of AIRS CO<sub>2</sub> between latitudes 30° S and 80° N.
- Here, we use the level 2 daily data from 1 January 2003 to 31 December 2016 as the studied period. Considering some days have no data in AIRS CO<sub>2</sub> product, we exclusively remove these days to generate our daily global data. As a result, there are 322 days left in every year and the total length is 14 X 322. To keep the density of nodes equally cover the globe (60°S to 80°N), the number of nodes we analyzed was normalized by the cosine of latitude.
- Therefore, AIRS data are interpolated into 2.5° 2.5° and the distance between neighboring nodes is around 830 km in both zonal and meridional directions. We analyze the daily data of CO<sub>2</sub> mapped to a subset of  $n = 658$  around the globe.

# The first network approach to CO<sub>2</sub>

- Because focusing on the coordination between locations rather than local dynamics, the network analysis methods always exhibit an increasing sensitivity to climate patterns which are not easily captured by conventional analysis (Feng and Dijkstra, 2014).
- Therefore, climate network methods provide a new perspective and paradigm for measuring the structural changes of climate networks, as well as the influence on remote regions.
- On the other hand, we know that CO<sub>2</sub> is very important in the climate system. However, there are no existing studies employing CO<sub>2</sub> within the framework of climate networks.

## 2.1. From climate data to networks

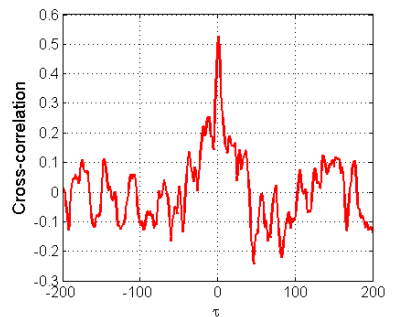
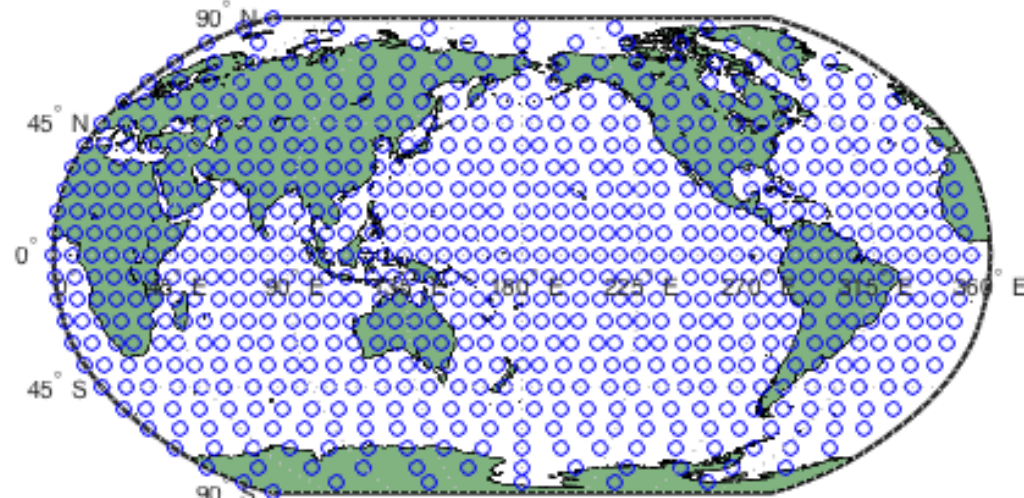
- Data set:
  - Daily NCEP/NCAR reanalysis data
  - 726 nodes of air temperature at 1000MB
  - Removal of seasonal cycle

- Definition of link weights:

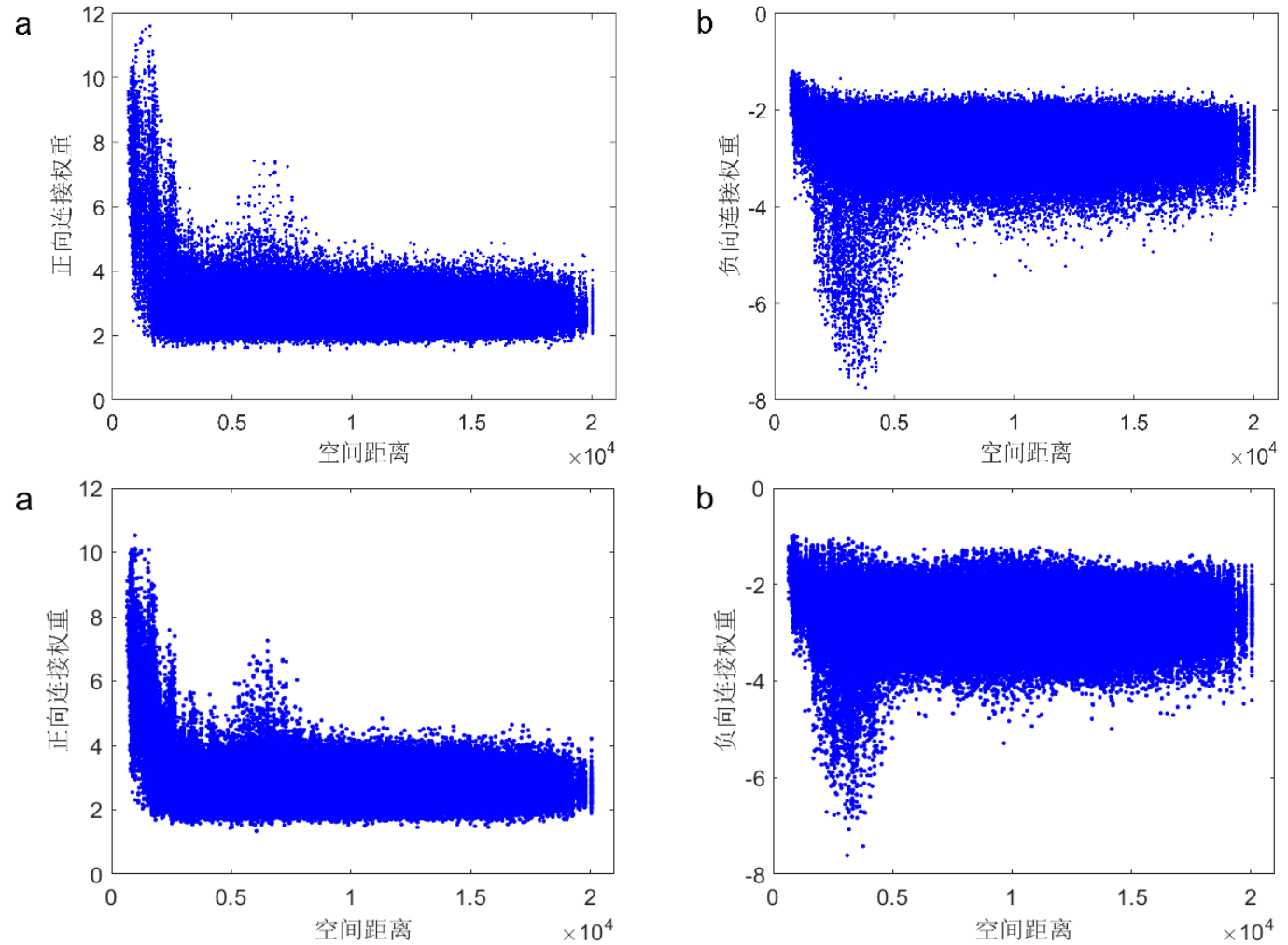
- Cross-correlation:  $X_{i,j}(\tau)$

- Positive link weights:  $W_{i,j}^{pos} = \frac{\max(X_{i,j}) - \text{mean}(X_{i,j})}{\text{std}(X_{i,j})}$ ; time delay:  $\tau_{i,j}^{pos}$

- Negative link weights:  $W_{i,j}^{neg} = \frac{\min(X_{i,j}) - \text{mean}(X_{i,j})}{\text{std}(X_{i,j})}$ ; time delay:  $\tau_{i,j}^{neg}$



# Results



# Results

- There is no significant difference between the original and shuffled data for either  $w_{i,j}^{neg}$  or  $P_{i,j}^{neg}$ .
- Therefore, we only focus on positive links.

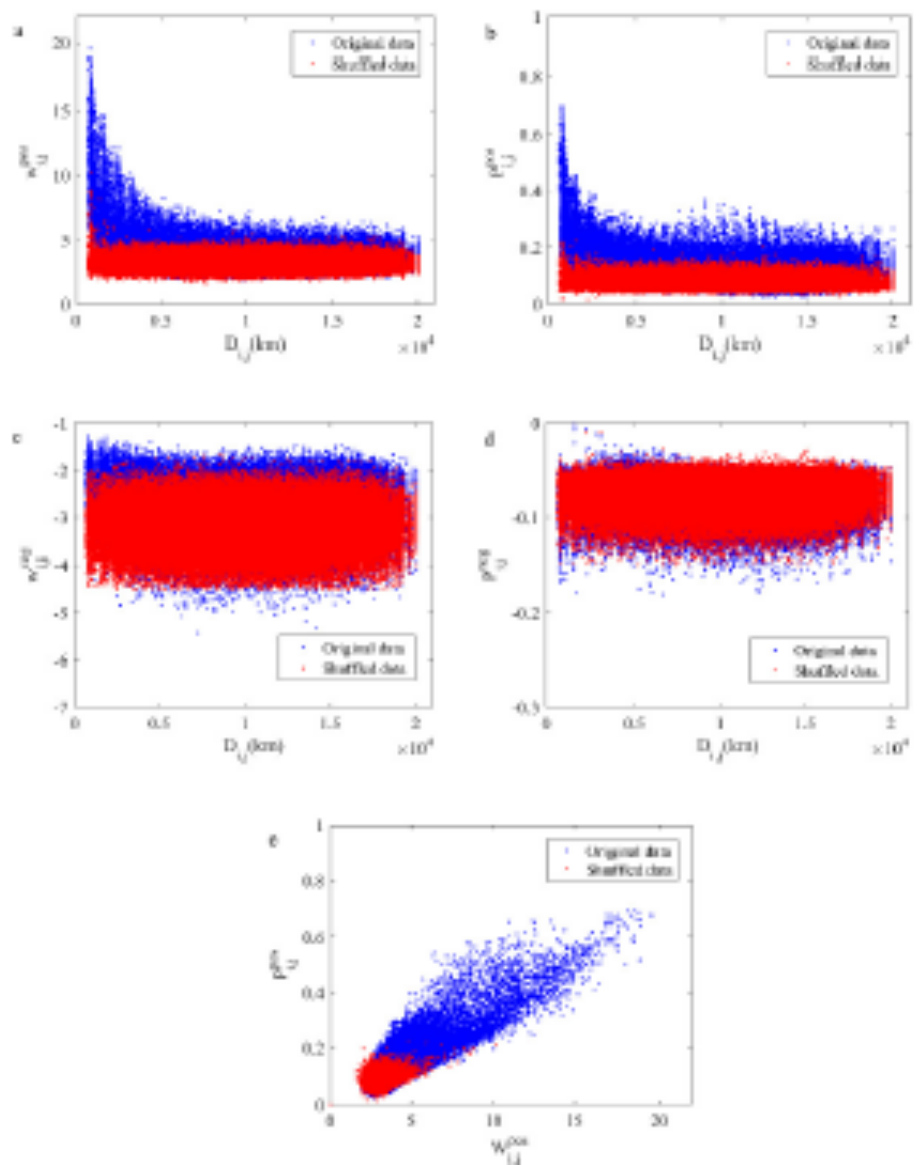
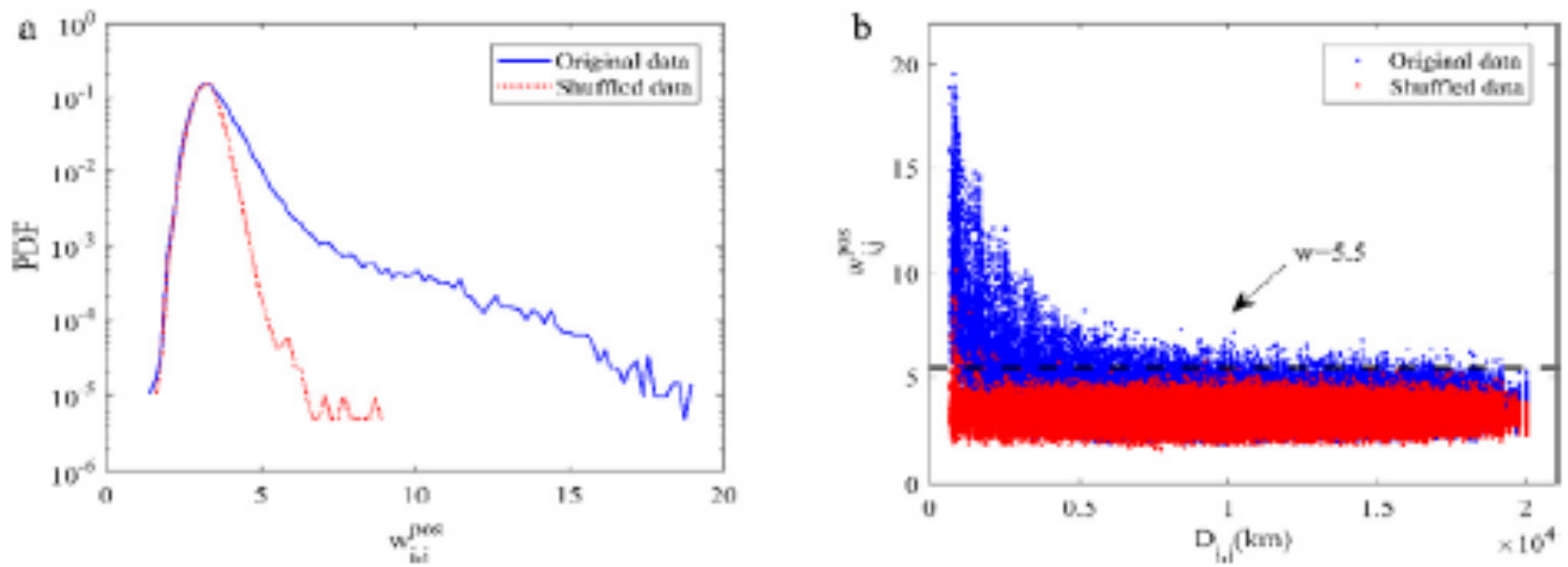


Fig. 2. (a) Positive link weights  $w_{i,j}^{pos}$  versus geographical distance  $D_{ij}$  for the original (blue dots) and shuffled (red dots) cases. (b) Maximum cross-correlation  $P_{i,j}^{pos}$  versus distance  $D_{ij}$  for the original (blue dots) and shuffled (red dots) cases. (c) Negative link weights  $w_{i,j}^{neg}$  versus distance  $D_{ij}$  for the original (blue dots) and shuffled (red dots) cases. (d) Minimum cross-correlation  $P_{i,j}^{neg}$  versus distance  $D_{ij}$  for the original (blue dots) and shuffled (red dots) cases. (e)  $P_{i,j}^{pos}$  vs  $w_{i,j}^{pos}$  for the original (blue dots) and shuffled (red dots) cases.

# Identifying significant links



**Fig. 3.** (a) PDF of the link weights for the original (blue line) and shuffled (red line) cases. (b) Positive link weights  $w_{ij}^{pos}$  versus distance  $D_{ij}$  for the original (blue dots) and shuffled (red dots) cases.

- 1, the observed link has a four-day time lag, propagating eastward from East Asia to the Northeastern Pacific Ocean and western North America. The obtained link follows the midlatitude winds (westerlies) in the region(Liang et al., 2004).
- 2 has a three-day time lag, and it is directed from North America to Mediterranean region and even North Africa. This link yields a clear connection with one of cross-Eurasia wave train linking North Atlantic to Eurasia (Ding and Wang, 2005) as well as North Atlantic storm track (Lan et al., 2017). Wave trains emerging from the southern part of the storm track in the North Atlantic transport to the Mediterranean region and subsequently propagate eastward along the subtropical westerly jet (Sung et al., 2006).
- 3 is the connection between the western Russia and southern China, in which the observed time delay is six days. It is probably consistent with the wave train pattern generated by NAO from the North Atlantic to East Asia (Zhu et al., 2011; Sun and Wang, 2012).
- 4 is a typical example of links along the southern hemisphere Rossby wave (Zhou et al., 2015), with five days of time delay.

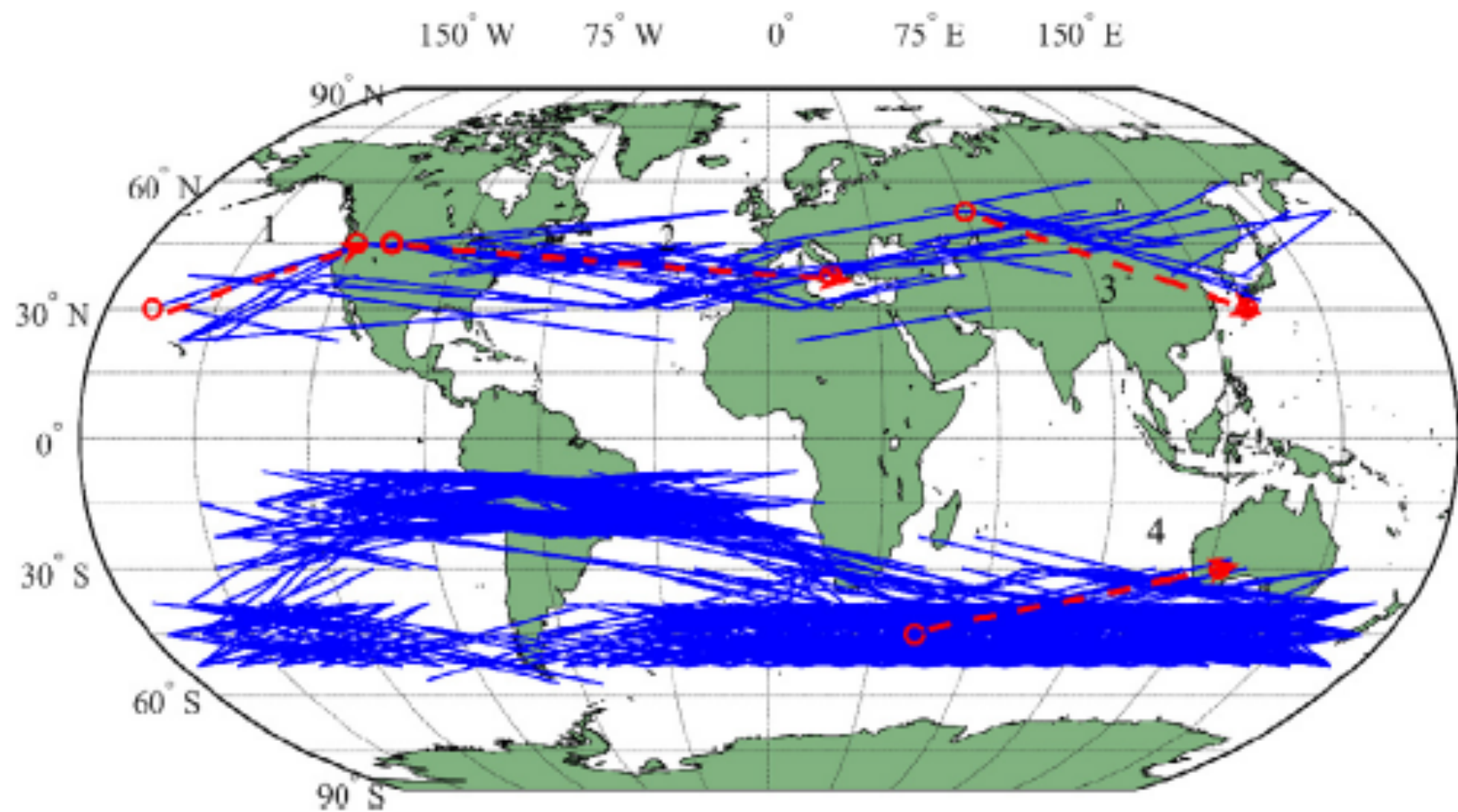


**Fig. 6.** Map of long-term positive links which have (i)  $D_{ij} \geq 3500$  km, (ii)  $w_{i,j}^{pos} \geq 5.5$  and (iii) latitude distance larger than  $5^\circ$ . The red circles and arrow dashed lines indicate the examples considered in the text.

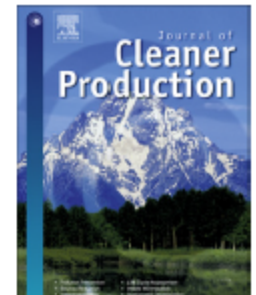


ELSEVIER

Contents lists available at ScienceDirect

## Journal of Cleaner Production

journal homepage: [www.elsevier.com/locate/jclepro](http://www.elsevier.com/locate/jclepro)



## Long-term link detection in the CO<sub>2</sub> concentration climate network

Na Ying <sup>a,\*</sup>, Dong Zhou <sup>b</sup>, Qinghua Chen <sup>c</sup>, Qian Ye <sup>a</sup>, Zhangang Han <sup>c</sup>



<sup>a</sup> Faculty of Geographical Science, Beijing Normal University, Beijing 100875, China

<sup>b</sup> Department of Physics, Bar-Ilan University, Ramat Gan 52900, Israel

<sup>c</sup> School of Systems Science, Beijing Normal University, Beijing 100875, China

# Nature letter Dec. 2018 paper on extreme rainfall teleconnections

- Climatic observables are often correlated across long spatial distances, and extreme events, such as heatwaves or floods, are typically assumed to be related to such teleconnections.
- Moreover, we uncover concise links between southcentral Asia and the European and North American extratropics, as well as the Southern Hemisphere extratropics. Analysis of the atmospheric conditions that lead to these teleconnections confirms Rossby waves as the physical mechanism underlying these global teleconnection patterns and emphasizes their crucial role in dynamical tropical–extratropical couplings.

LETTER

<https://doi.org/10.1038/s41586-018-0872-x>

## Complex networks reveal global pattern of extreme–rainfall teleconnections

Niklas Boers<sup>1,2\*</sup>, Bedartha Goswami<sup>2,7</sup>, Aljoscha Rheinwalt<sup>3,7</sup>, Bodo Bookhagen<sup>3</sup>, Brian Hoskins<sup>1,4</sup> & Jürgen Kurths<sup>2,5,6</sup>

# Hainan Province Natural Hazard Infrastructure Network Function Risk Assessment and Recovery Research

# Background

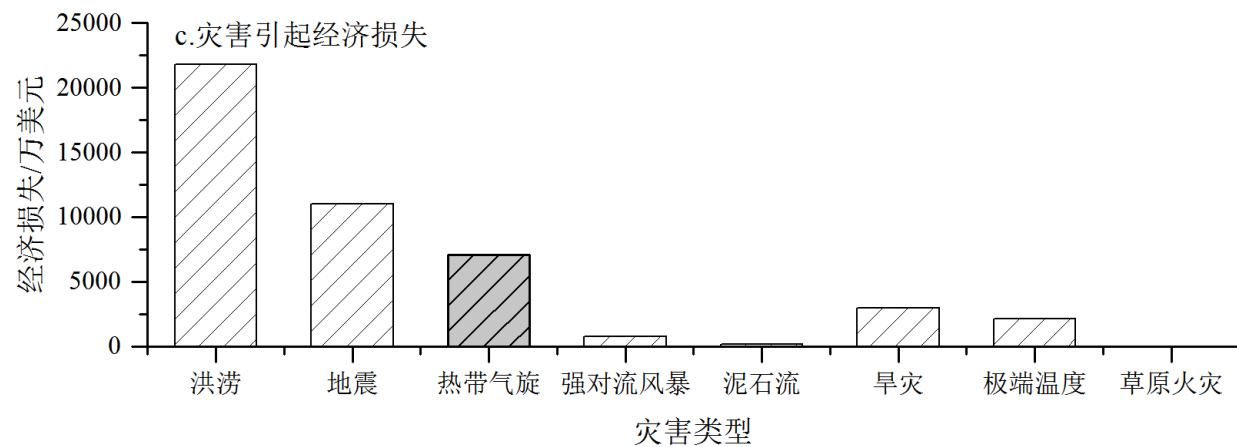
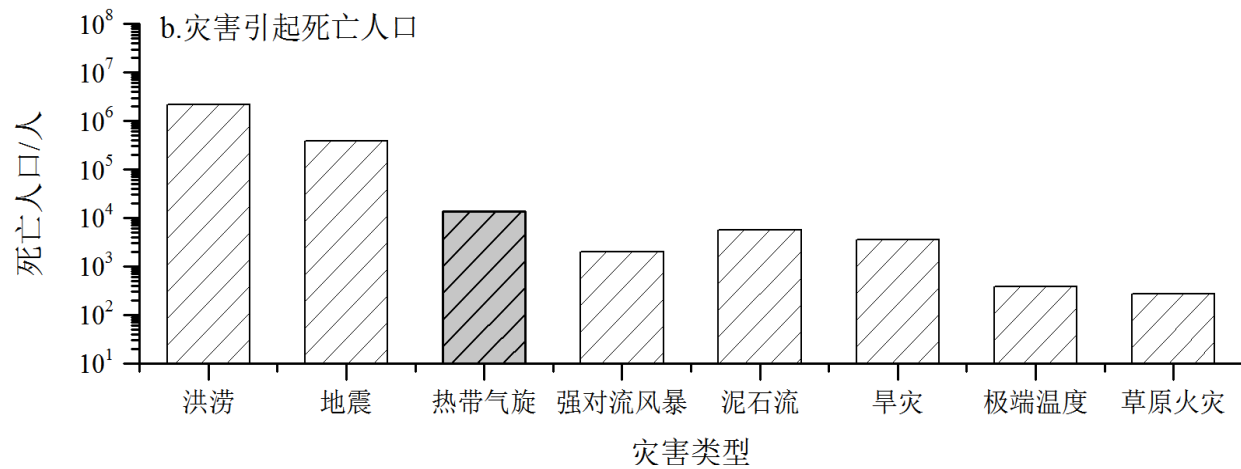
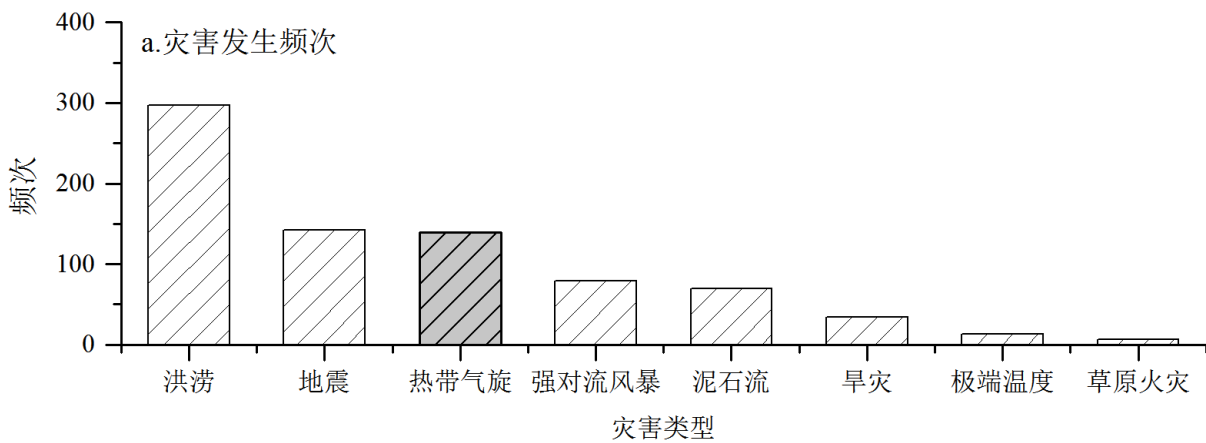


图1-4 1960-2014年中国不同灾害发生频次、造成人口死亡和经济损失状况（数据源：EM-DAT）

# Background

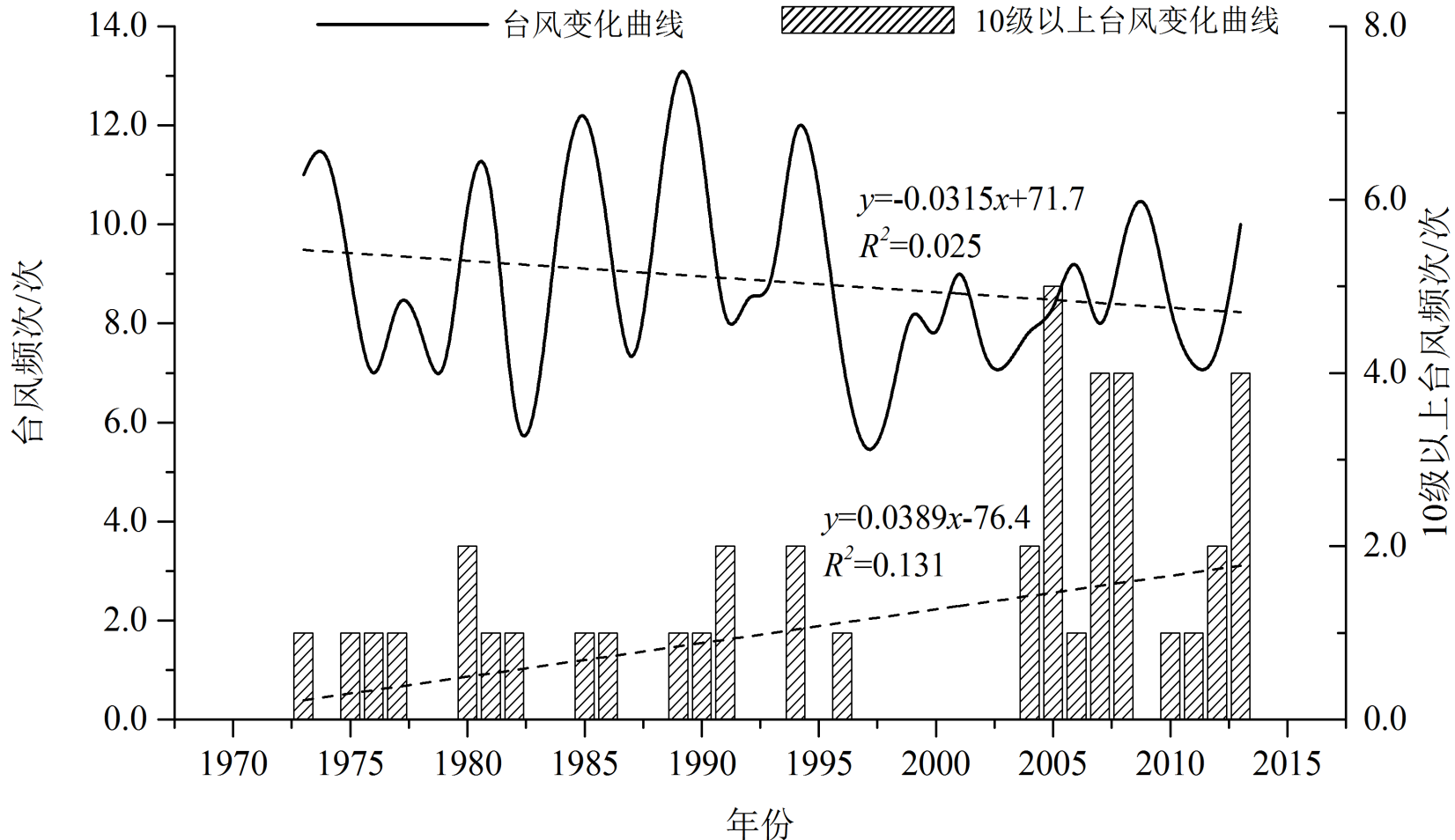


图1- 5 1973-2013年登陆中国的10级以上台风年频数  
(数据源: 中国气象局提供的西北太平洋的热带气旋最佳路径数据集)

# Background



(A)



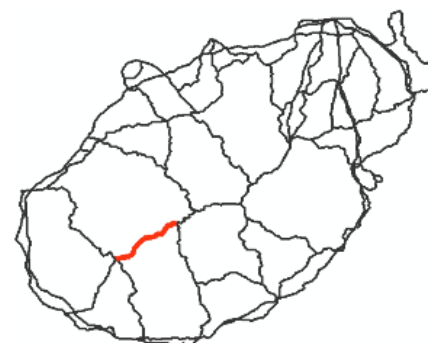
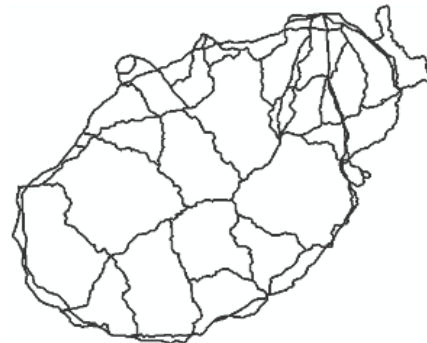
(B)

图 (1) 台风“威马逊”对道路的损害 (A) 道路旁边的行树倒伏 (B) 路面塌陷 (来源：由海口市市政管理局编制的《威马逊台风对海口市主城区市政设施的影响评估及对策分析》)

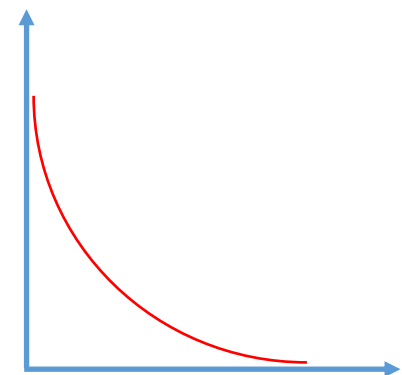
## 研究层面

网络（整体）

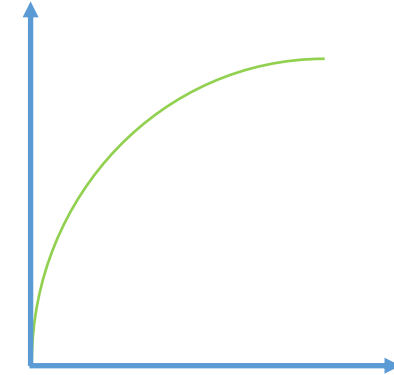
组件（个体）



## 研究角度



风险评估



恢复性提升

研究情景：自然灾害



网络风险评估

组件风险贡献

网络优化恢复



图 海南岛地理位置以及历史台风路径

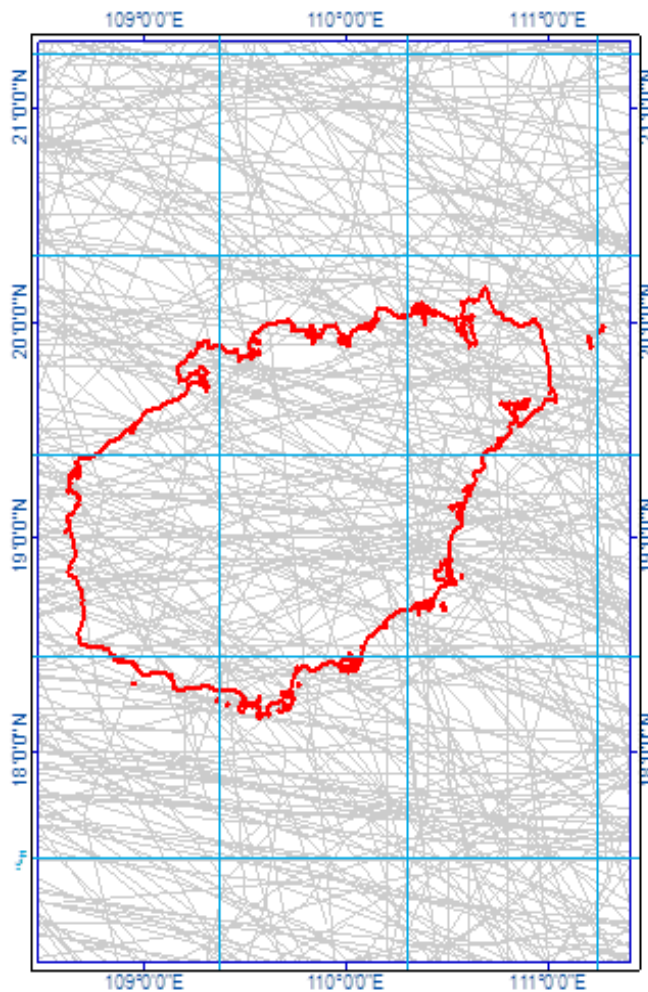
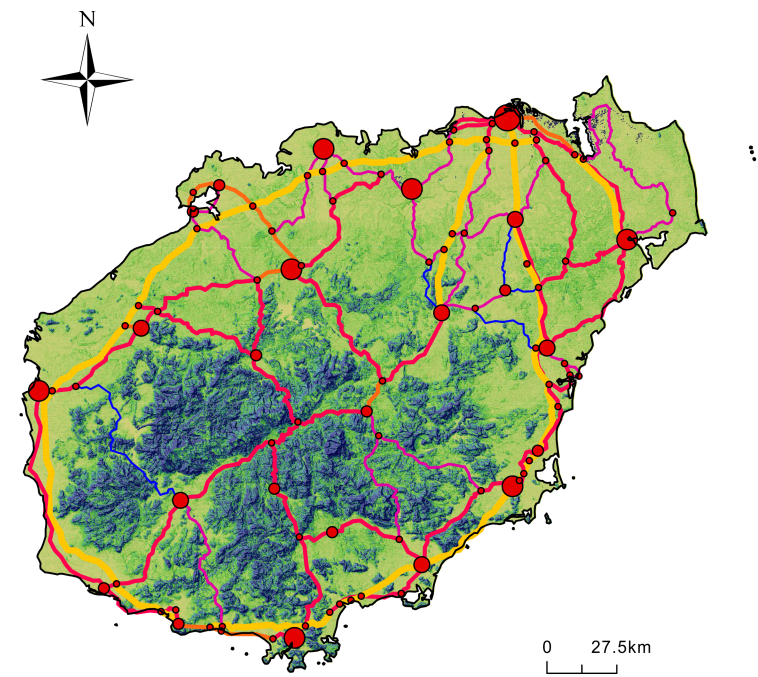


图 海南岛公路网



图例

人口 (万人)	道路等级				
	0.0 - 6.2	6.2 - 17.7	17.7 - 37.8	37.8 - 66.0	66.0 - 217.1
●	高速公路	一级道路	二级道路	三级道路	四级道路

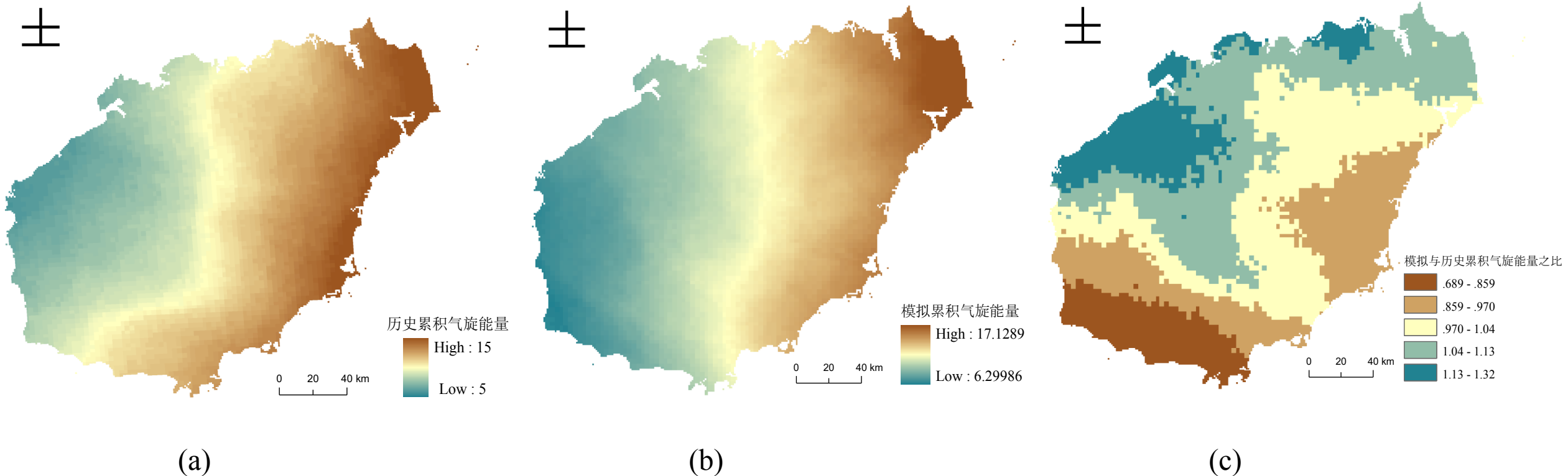
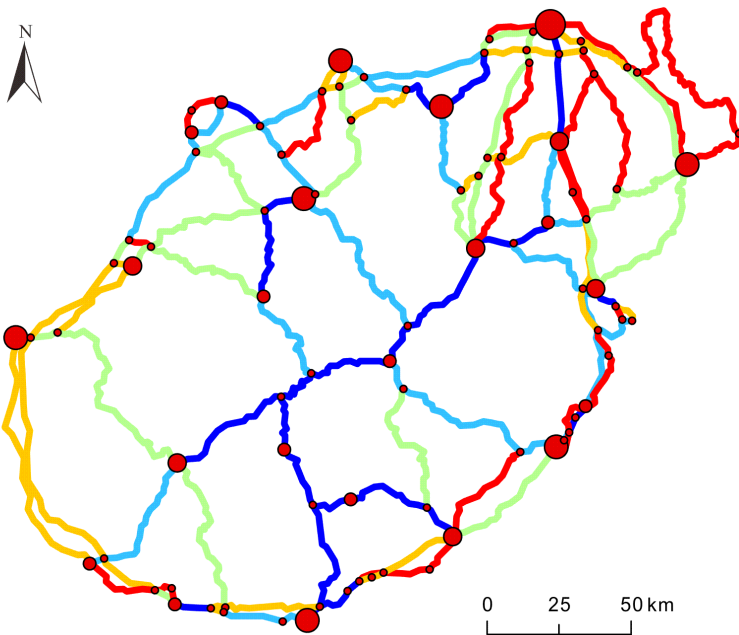


图2-12海南岛历史和模拟台风的累积气旋能量空间分布

(a) 历史累积气旋能量 (b) 模拟累积气旋能量 (c) 模拟与历史累积气旋能量的比值 ( $0.25^\circ \times 0.25^\circ$ )

a. 距离效益损失贡献



b. 旅行延误贡献

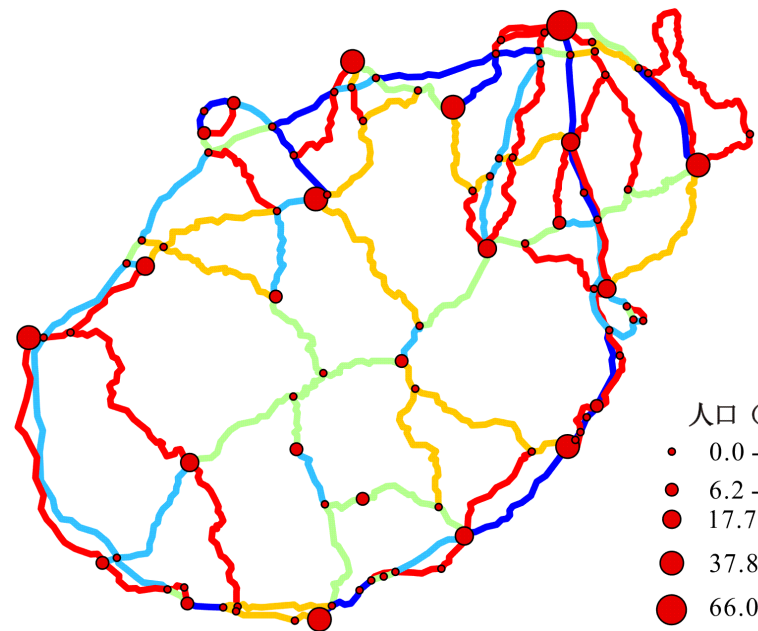


图4-3单路段受损情景下路段功能损失贡献空间格局

# 自然灾害基础设施恢复性研究

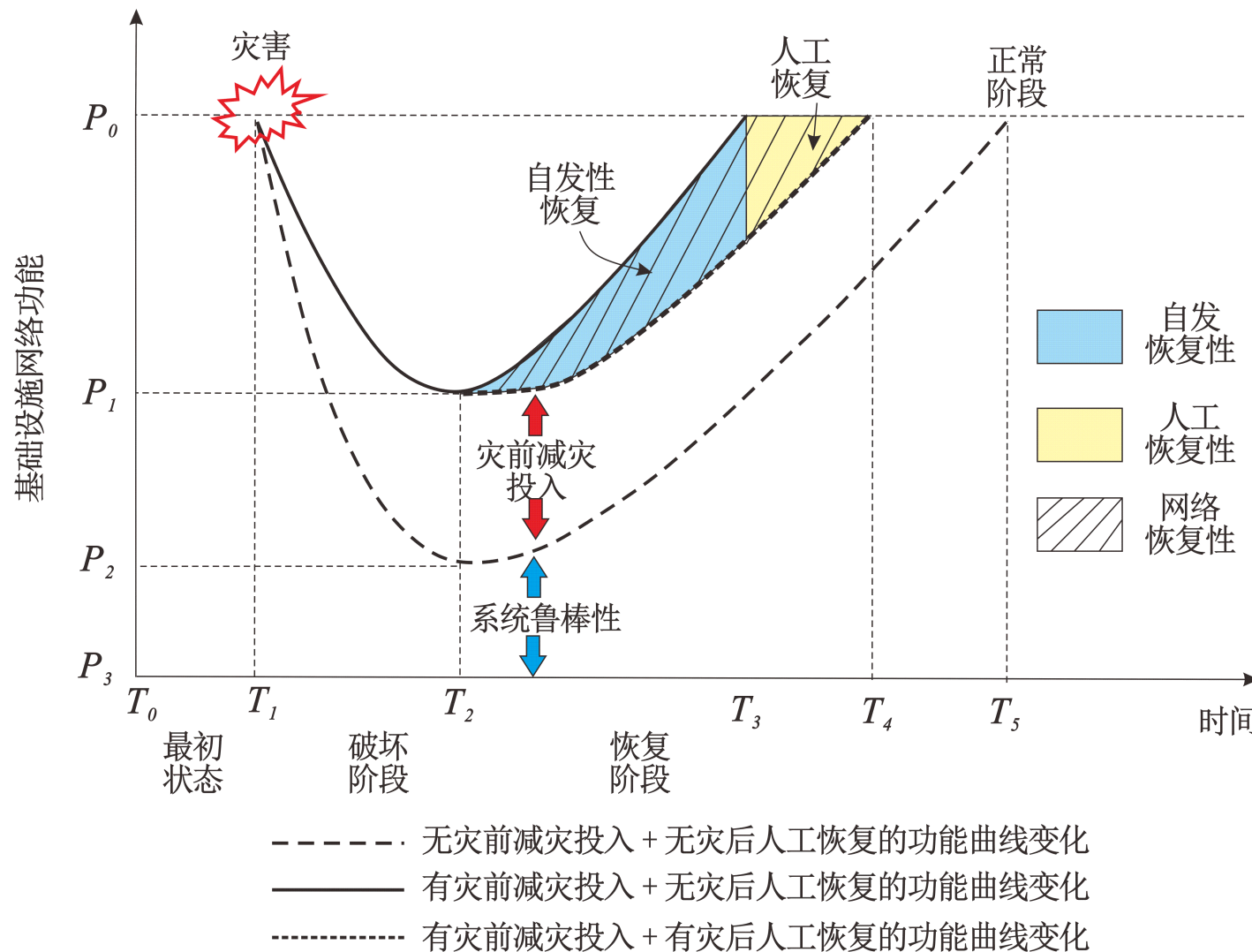


图1- 2 基础设施网络从遭受灾害影响到最终完全恢复的过程

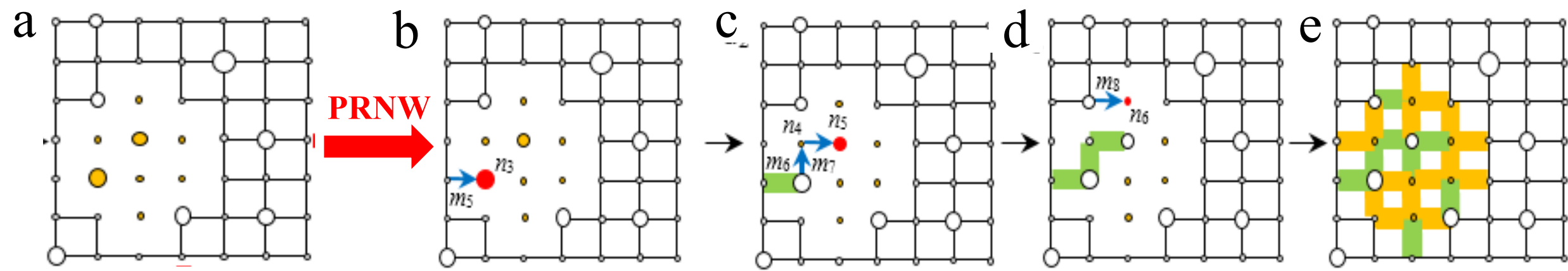


图5-1 格型网络在局部破坏之下偏好恢复策略的操作过程

# Road Function Recovery Simulation

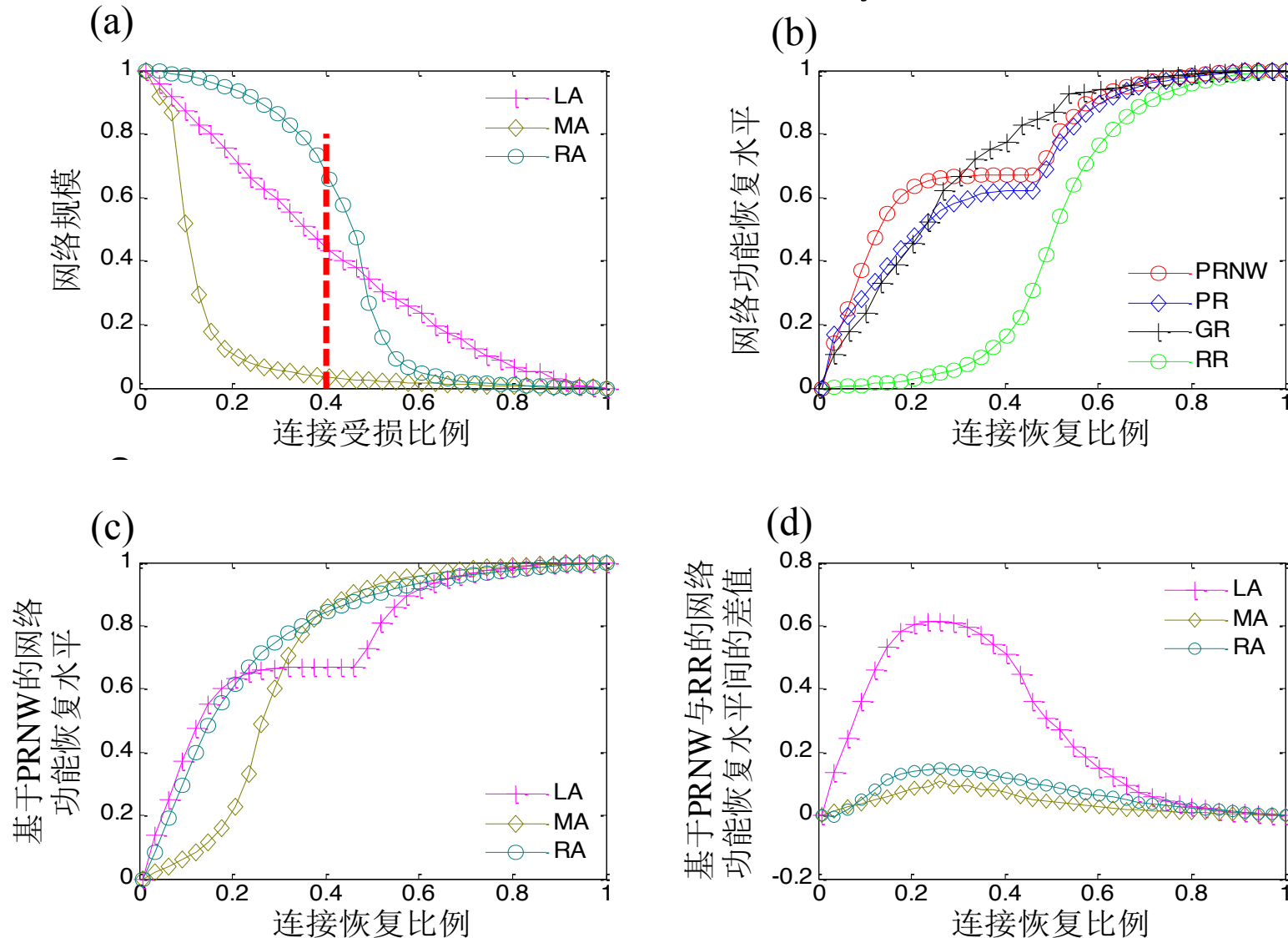
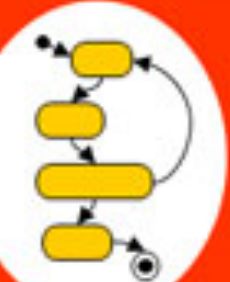
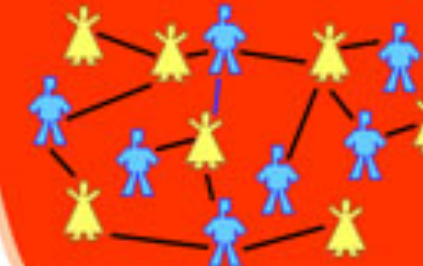


图5-4异质格型网络受破坏过程与功能恢复过程仿真结果

An agent-based modeling  
approach for housing prices

# Why agent-based modeling?

## Agent Based Modeling

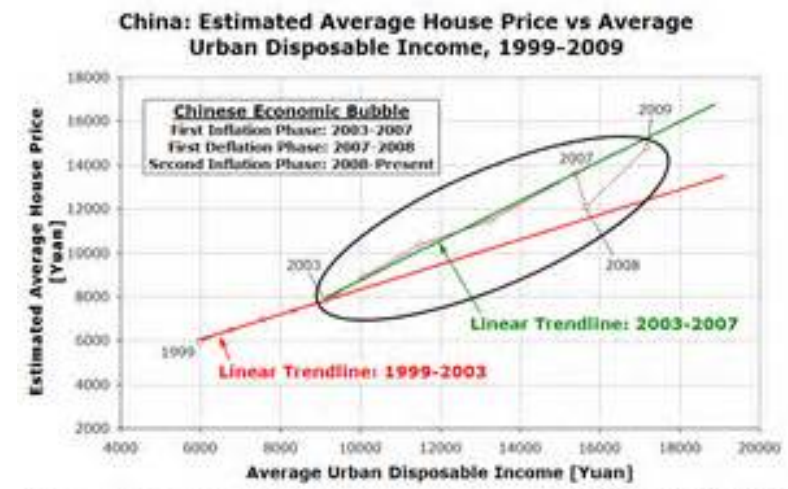


- Disaster is a complex system.
- An **agent-based model (ABM)** can simulate the actions and interactions of autonomous with a view to assessing their effects on the system as a whole.
- Adaptability to game theory, complex systems, emergence, computational sociology, multi-agent systems, and evolutionary programming.

# Why housing prices?



- A typical assets
- A sensitivity index of economy, disaster impact, and societal satisfaction
- Existing research

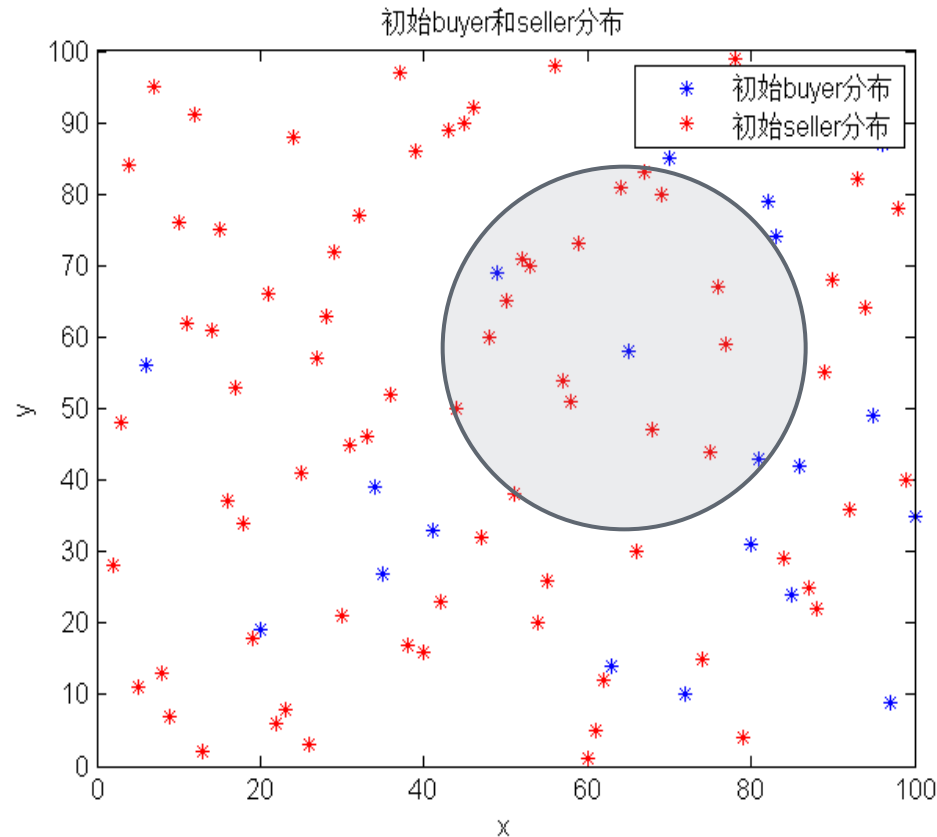


# The proposed model

- **Bounded rationality, iterative, agent-based model**
  - Incomplete information
  - Option pool
  - Evolution mechanism
  - Emotional factor

# Incomplete Information

- Definition of neighborhood
  - Euclidean space
  - Euclidean distance
  - Radius= 25, 50, 100
- Definition of expiration
  - t=12 months



# Option Pool



- **Option pool for sellers**

- The price with the largest sales of his own in last 12 months;
- The price with the largest “suitability”<sup>1</sup> in neighborhood in last 12 months;
- The maximum weighted average price<sup>2</sup> in last 12 months;
- The maximum of the prices of options 1-3.

- **Option pool for buyers**

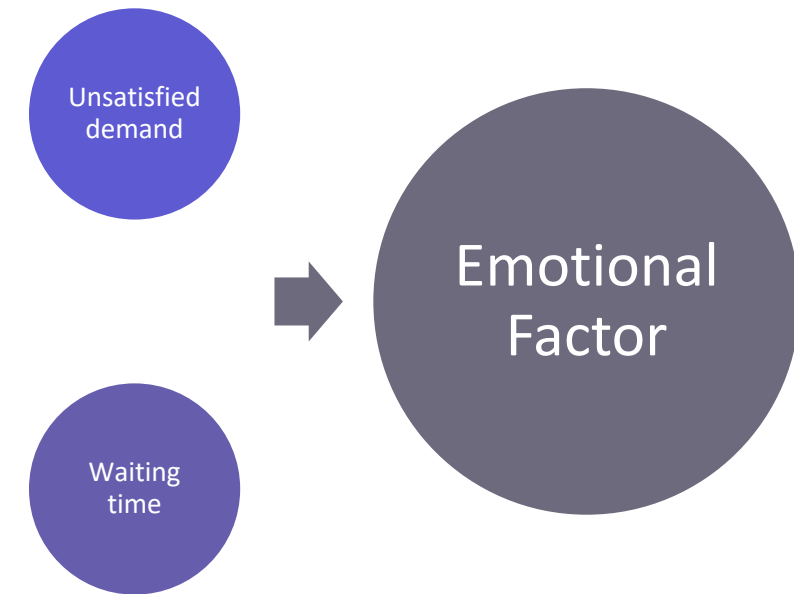
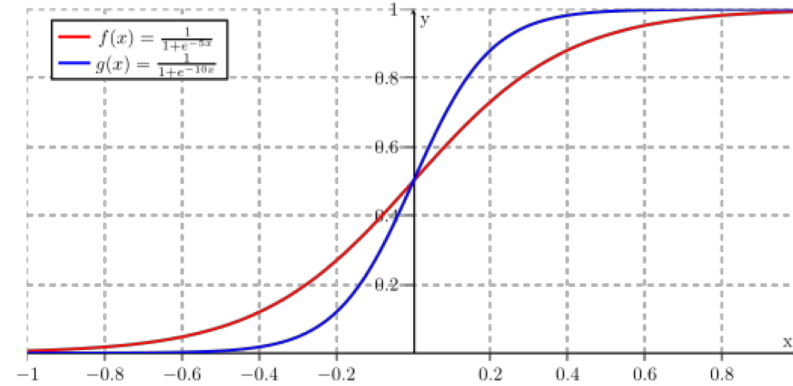
- As same as the last month’s strategy;
- As same as the average of last 12 months;
- As same as the projected price based on last year’s data;
- As same as the average of last 4 months;
- As same as the average of last 6 months.

# Evolution Mechanism

- The perception of a “good price” or good strategy will increase the possibility of using this price or strategy.
- $(1,1,1,1) \rightarrow (1,2,1,1) \rightarrow \dots \rightarrow (n_1, n_2, n_3, n_4)$

# Emotional factor

- Sigmoid function
- Unsatisfied demand
- Time factor



# Input data

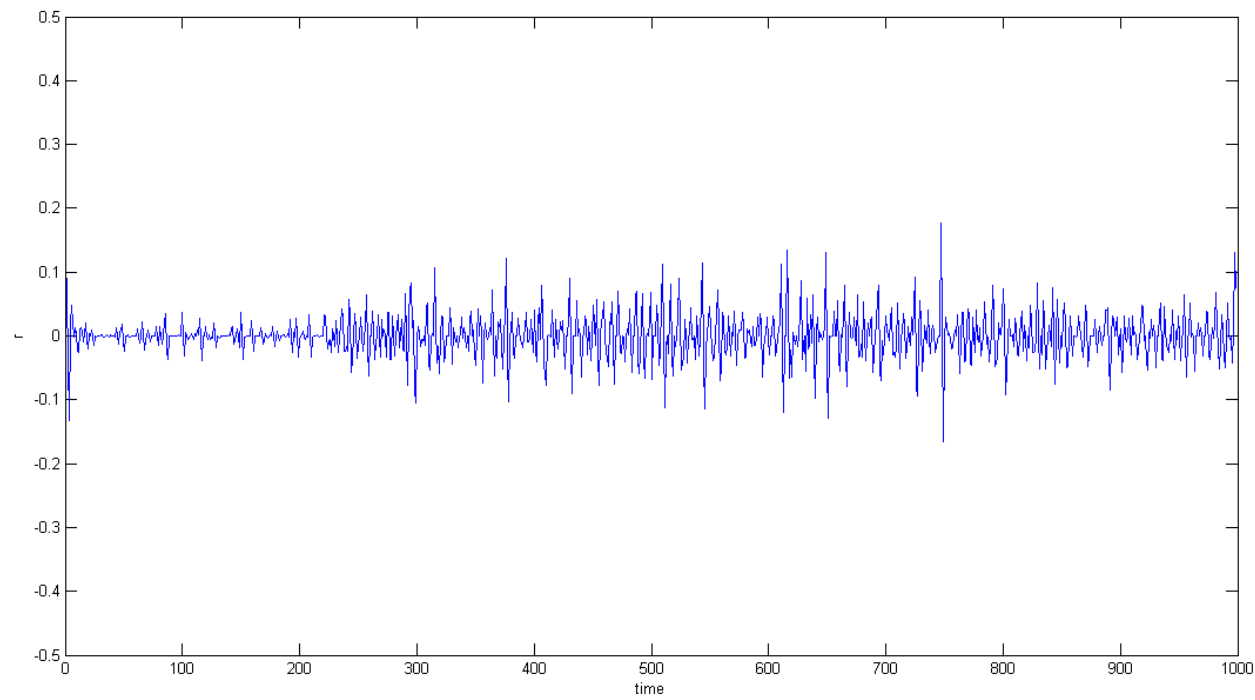
- Real world monthly housing price in Shanghai, 2013
- $T=5000$
- #Buyer=80
- #Seller=20
- Size of memory =12
- Size of option pool for seller =4
- Size of option pool for buyer =5

# Stylized empirical facts

- A simplified presentation of an empirical finding
- Stylized Facts for Financial Returns
  - distributional properties
  - tail properties
  - extreme fluctuations
  - pathwise regularity
  - linear and nonlinear dependence of returns
  - . . .

# Price Return

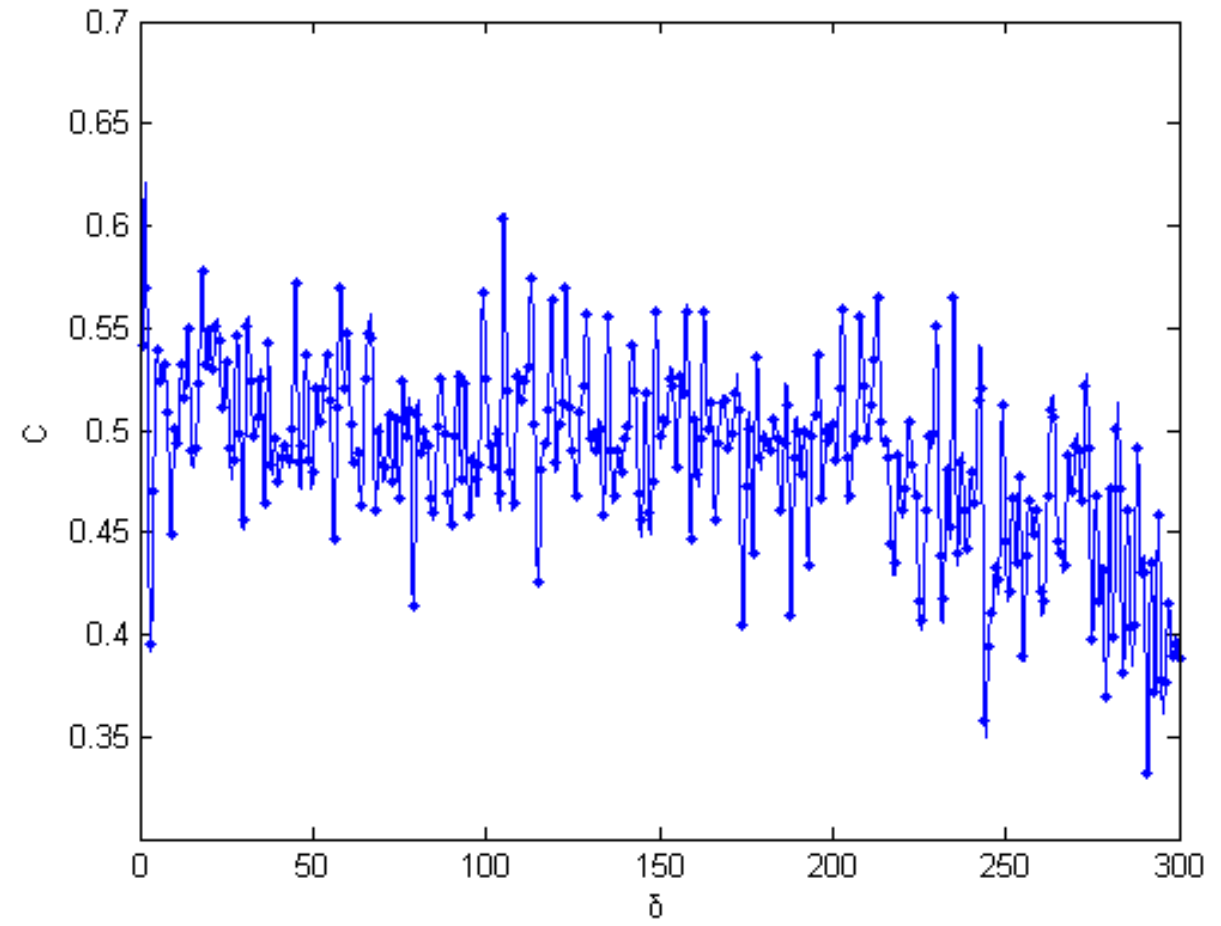
$$r(t) = \log P_t - \log P_{t-\delta}$$



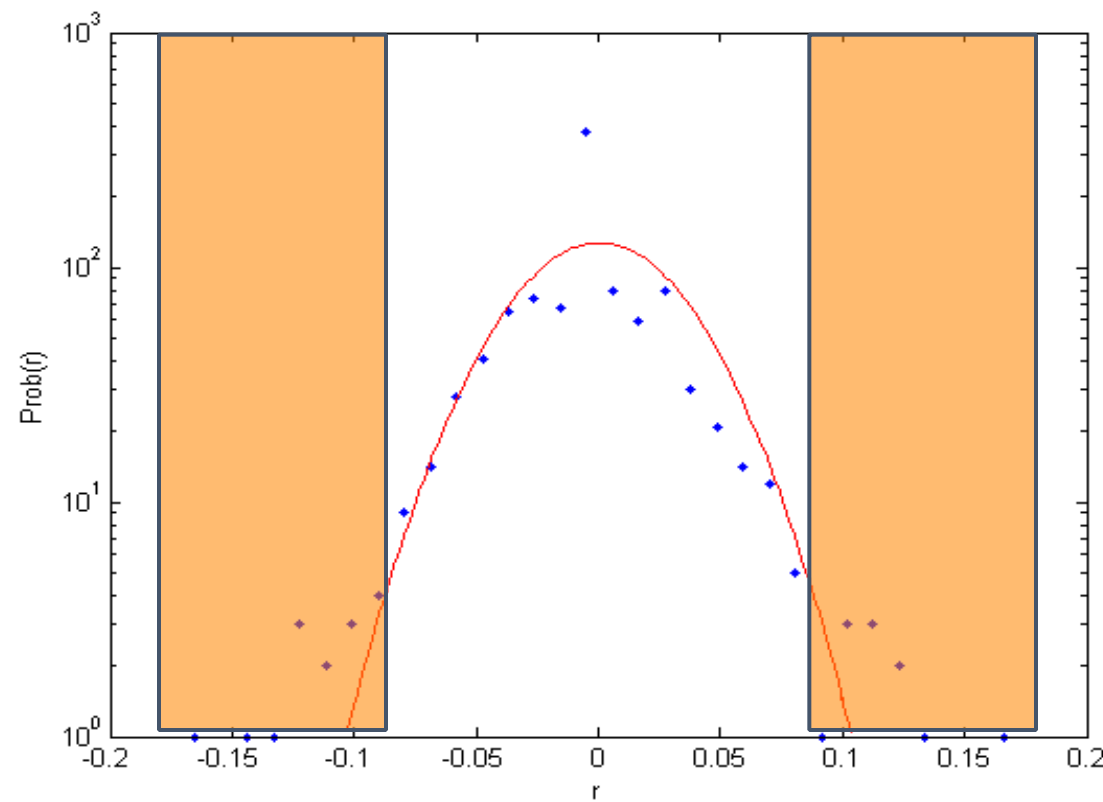
# Stylized Facts 1: Absence of autocorrelations

- Return autocorrelation:

$$C(\delta) = \frac{\langle r(t+\delta)r(t) \rangle - \langle r(t+\delta) \rangle \langle r(t) \rangle}{\langle r^2(t) \rangle}$$

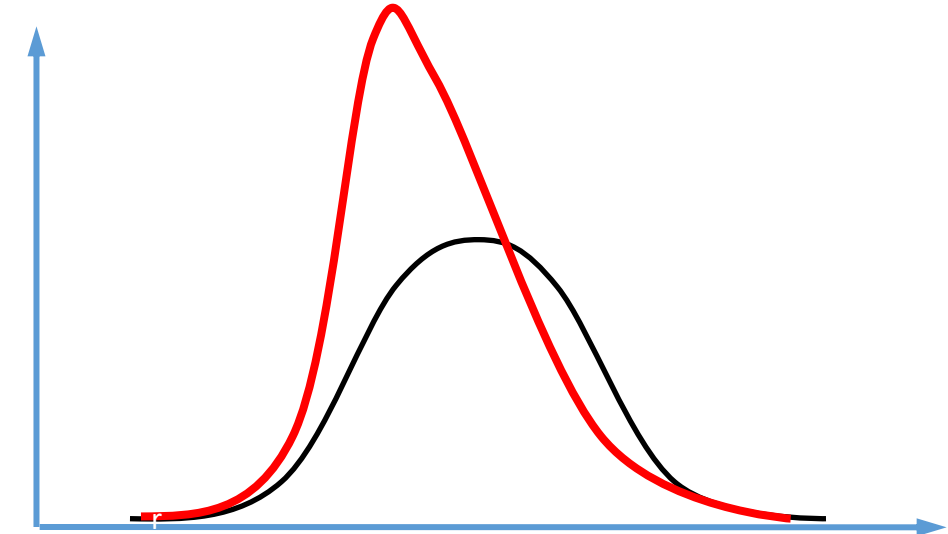


# Stylized Facts 2: Heavy tails



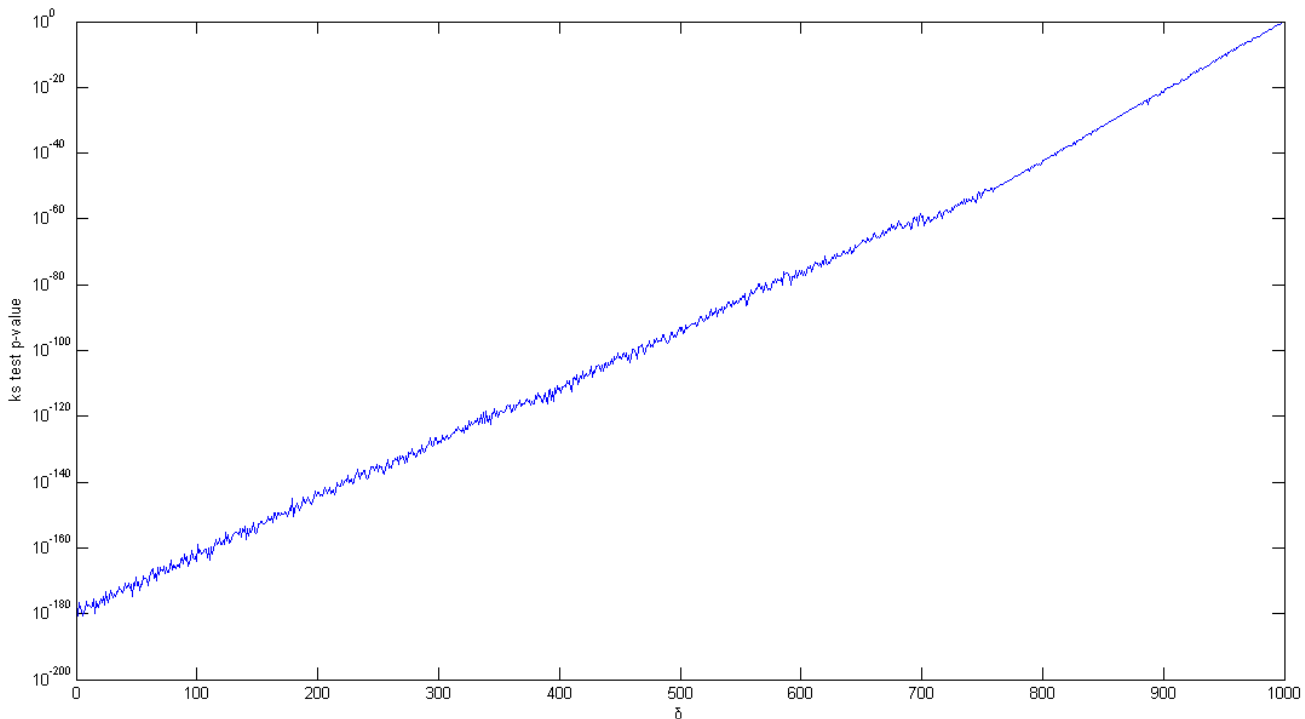
## Stylized Facts 3: Gain/Loss asymmetry

- Skewedness of a normal distribution =0
- Kurtosis of a normal distribution =3
- Skewedness of simulated results= 0.1225
- Kurtosis of simulated results =6.2803



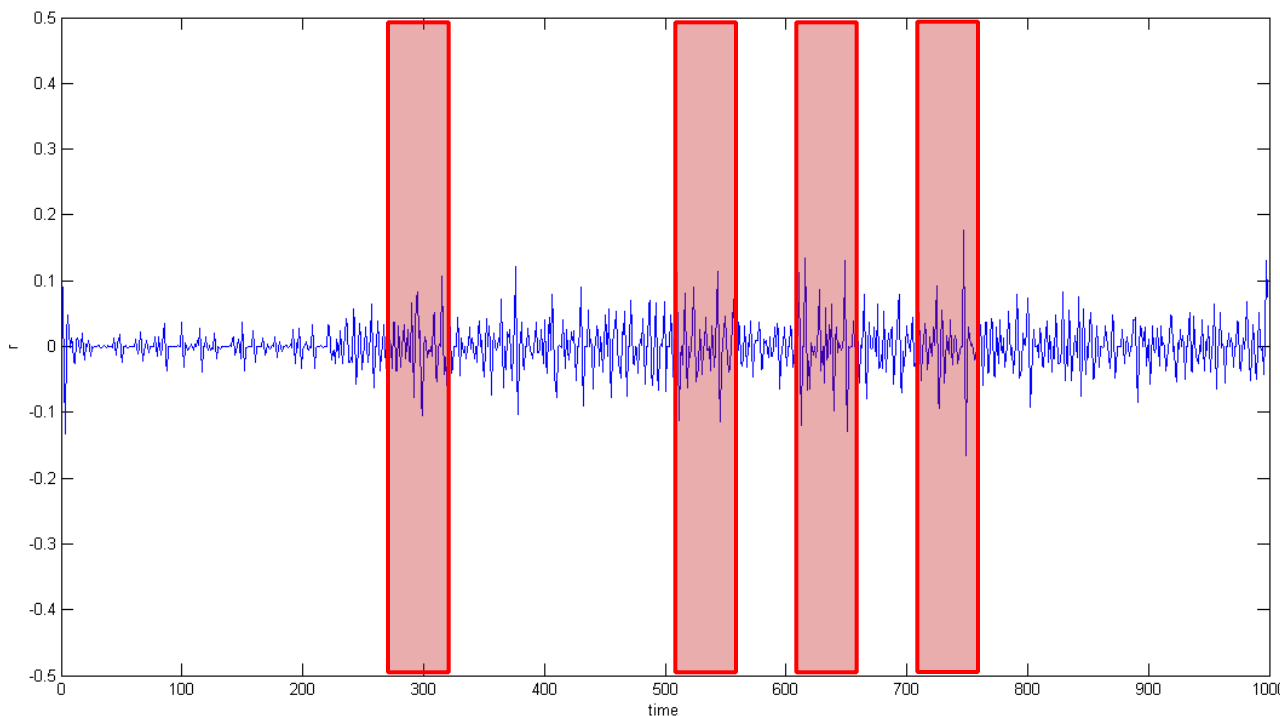
# Stylized Facts 4: Aggregational Gaussianity

- “As one increases the time scale over which returns are calculated, their distribution looks more and more like a normal distribution”.(Cont, 2001)

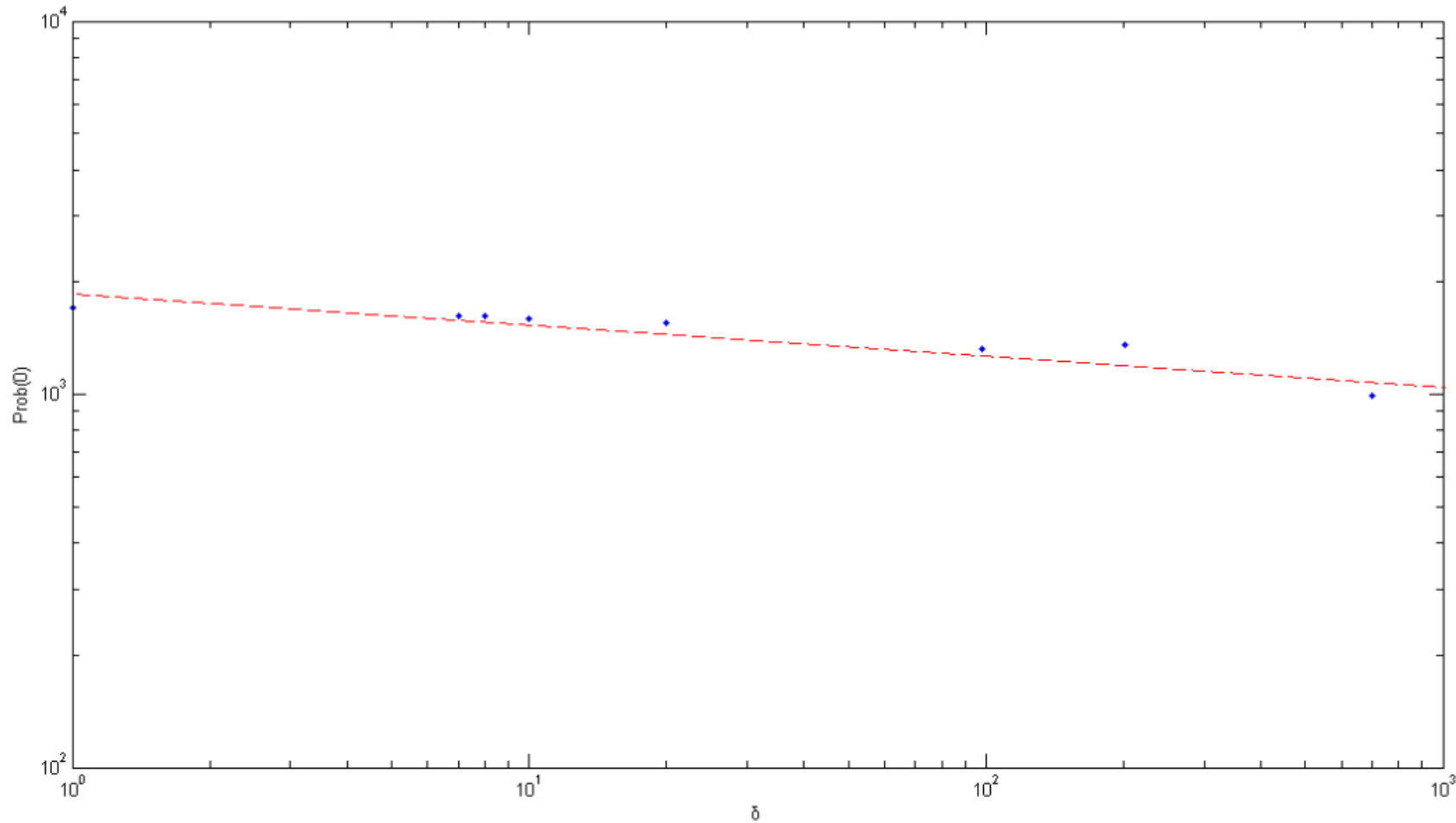


# Stylized Facts 5: Volatility clustering

- Large price variations are more likely to be followed by large price variations.

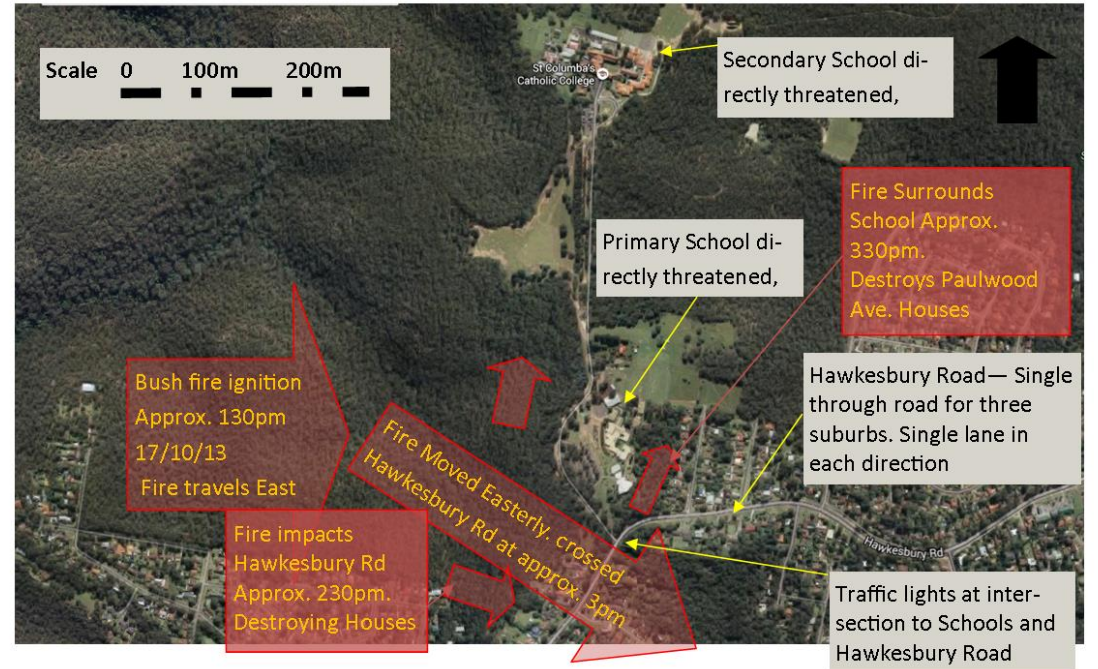
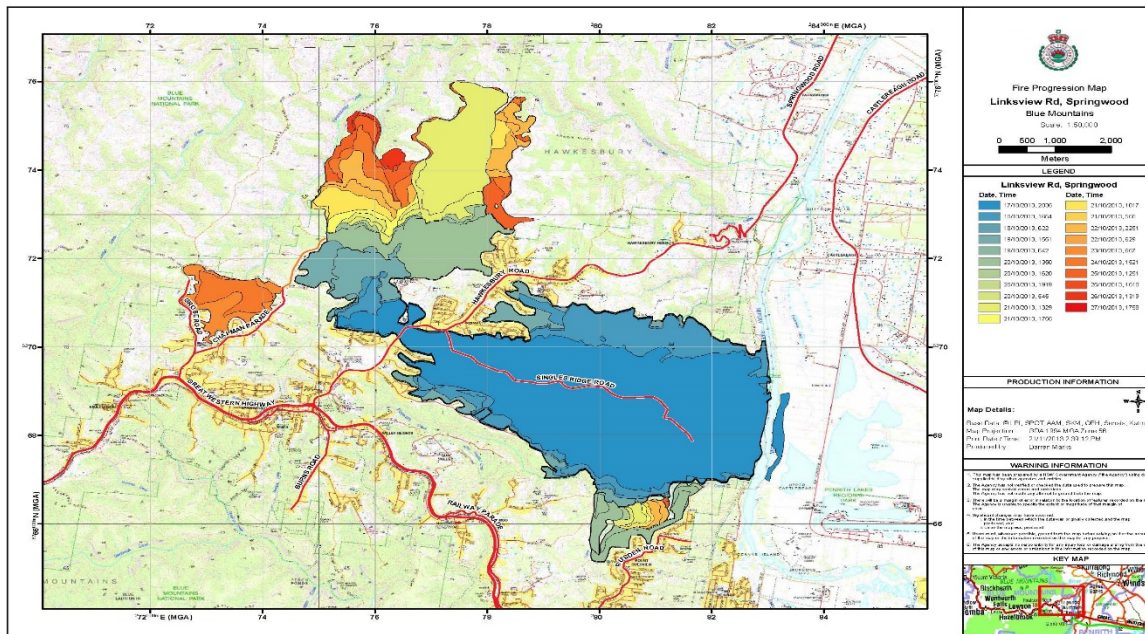


# Stylized Facts 6: Scaling Behavior



# Modelling solutions to improve resilience in disaster scenarios

- The bushfire disaster in the Blue Mountains in 2013



Thank you